

Supporting Information for

Effects of Ligand and Guest Solvent Molecule on Luminescent Property of Tb:Eu-Codoped Indium-Based MOF

Wenbo Yan, Le Wang, Kete Yangxiao, Zhixing Fu and Tao Wu*

State and Local Joint Engineering Laboratory for Novel Functional Polymeric Materials; College of
Chemistry, Chemical Engineering and Materials Science, Soochow University, Jiangsu 215123,
China

Table of Contents

1. Materials and general procedures
2. Syntheses of **1** and **2**
3. PXRD patterns (**Figure S1-S2**)
4. Structure of **2** (**Figure S3**)
5. TGA curves (**Figures S4**)
6. ICP and EDS measurement of **1** and **2** (**Table S1**)
7. EDS mapping of **2** (**Figure S5**)
8. Calculation of the triplet state of TATB ligand (**Figure S6**)
9. Fluorescent photograph of **1** soaked in different organic solvents (**Figure S7**)
10. Gas sorption measurement of compound **2** (**Figure S8**)

1. Materials and general procedures

All chemicals were used without any further purification. Powder X-ray diffraction (PXRD) data were collected on the Bruker D2 Phaser diffractometer by using Mo K α ($\lambda = 0.71073 \text{ \AA}$) radiation. The calculated PXRD patterns were produced by using the Mercury program and single crystal data. Thermogravimetric analyses (TGA) were carried out in an N₂ atmosphere with a heating rate of 10°C/min on a Shimadzu TGA-50 thermal analyzer. Energy dispersive spectroscopy (EDS) analyses were performed on scanning electron microscope (SEM) equipped with energy dispersive spectroscopy (EDS) detector. The PL spectra were collected on an HORIBA scientific Fluorolog-3 steady state and time-resolved fluorescence spectrophotometer equipped with a 450 W xenon lamp. The EDS mapping were carried on ZEISS EVO-18. Inductive Coupled Plasma Emission Spectrometer (ICP) is measured on inductively coupled plasma mass spectrometry with a Thermo Finnigan high resolution magnetic sector Element 2.

2. Synthesis

2.1 Synthesis of **1**

A mixture of In(NO₃)₃·*n*H₂O (0.25 mmol, 100 mg), Eu(NO₃)₃·6H₂O (*x* mmol, *x*=0, 0.0035, 0.007, 0.014, 0.028, 0.042, 0.056, 0.07, 0.084, 0.098, 0.112, 0.126 and 0.14, respectively), Tb(NO₃)₃·6H₂O (0.14-*x* mmol), H₃TATB (0.0227 mmol, 10 mg) was dissolved in 2.6 mL DMF and 0.1 mL DI water, and loaded into a 20 mL glass tube. The mixture was then heated to 100°C and kept for 5 days. After slowly cooling down to room temperature, colorless crystals were obtained.

(Note: crystal quality of **1** is not good enough to determine the structure from single-crystal x-ray diffraction data, however, the powder XRD data match well with simulated XRD pattern of CPM-19, which indicates that **1** is iso-structural with CPM-19.)

2.2 Synthesis of **2**

A mixture of In(NO₃)₃·*x*H₂O (0.45 mmol, 180 mg), Eu(NO₃)₃·6H₂O (*x* mmol, *x*=0, 0.005, 0.01, 0.015, 0.02, 0.025, 0.03, 0.035, 0.04, 0.045 and 0.05, respectively), Tb(NO₃)₃·6H₂O (0.05-*x* mmol), H₃BTC (0.4 mmol, 80 mg) was dissolved in 4 mL DMF and 1 mL DI water, and loaded into a 20 mL glass bottle. The mixture was then heated to 120°C and kept for 5 days. After slowly cooling down to room temperature, colorless crystals were obtained.

3 PXRD patterns

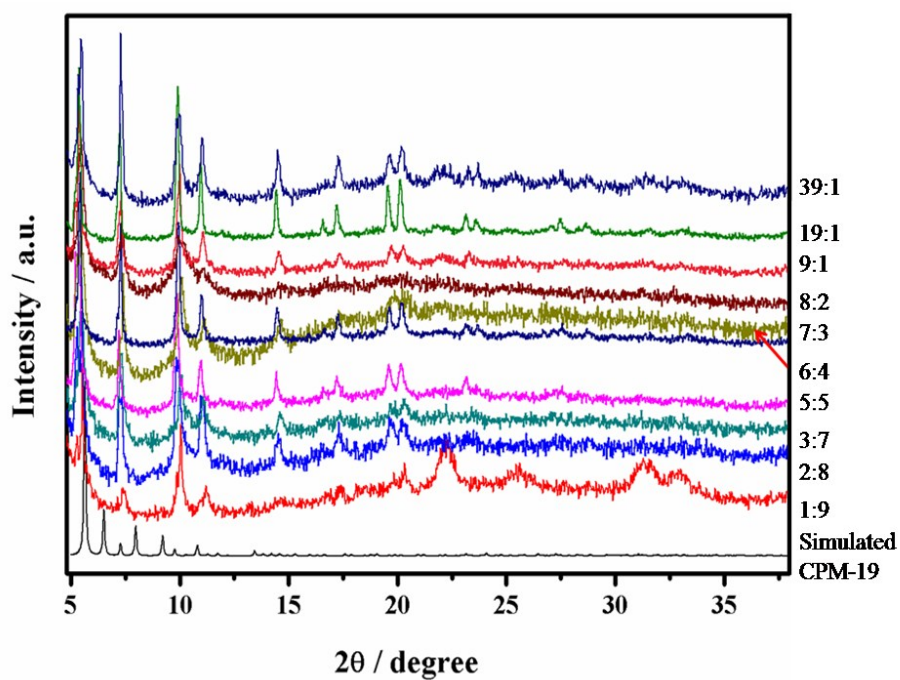


Figure S1. XRD patterns of Ln-In-TATB (1) with different Tb:Eu ratio.

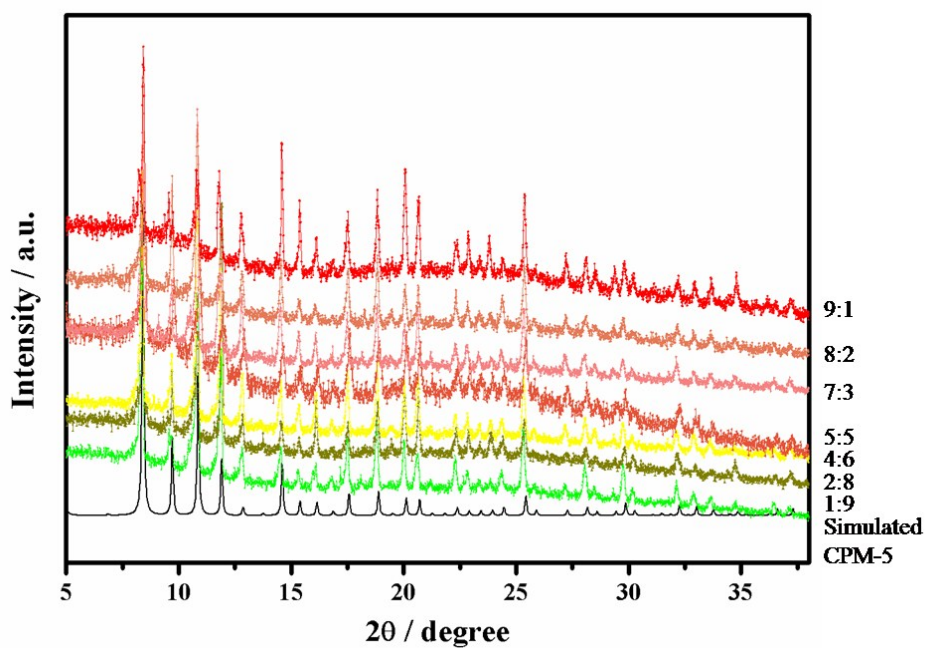


Figure S2. XRD patterns of Ln-In-BTC (2) with different Tb:Eu ratio.

4 Structure of 2

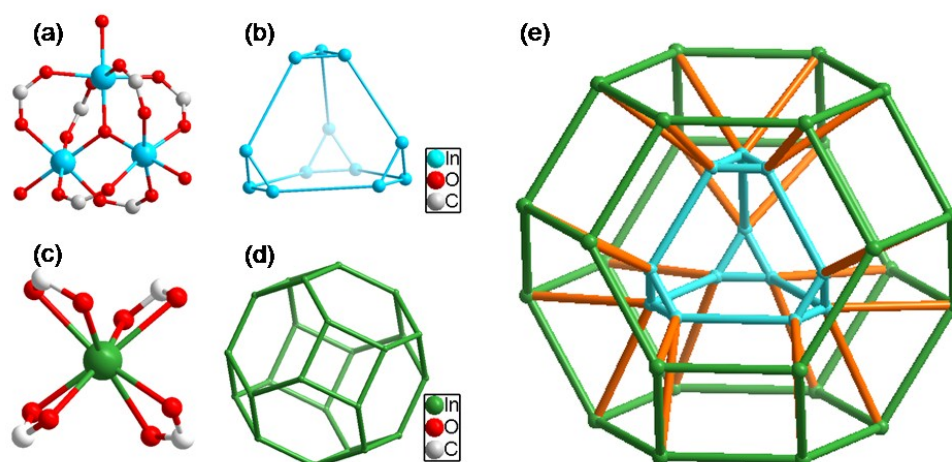


Figure S3. Structure of Ln-In-BTC(2). (a) The SUBs of the inter cage. (b) Ball-and-stick model of the inter cage. (c) The SUBs of the outer cage. (d) Ball-and-stick model of the outer cage. (e) Ball-and-stick model of Ln-In-BTC.

CPM-5 is cage-in-cage structure. The indium ions in the inter cage adopts 6-coordination model. The Indium ions in the outer cage adopts 8-coordination model, which is quite similar to the coordination model of lanthanide ions and offers the opportunity for doping lanthanide ions into CPM-5. Of course, the cage-in-cage structure makes CPM-5 possessing large porosity. By in-situ doping method, the structure as well as the luminescent properties of dual-lanthanide-doped CPM-5 can be well controlled.

5 TGA data of 1 and 2

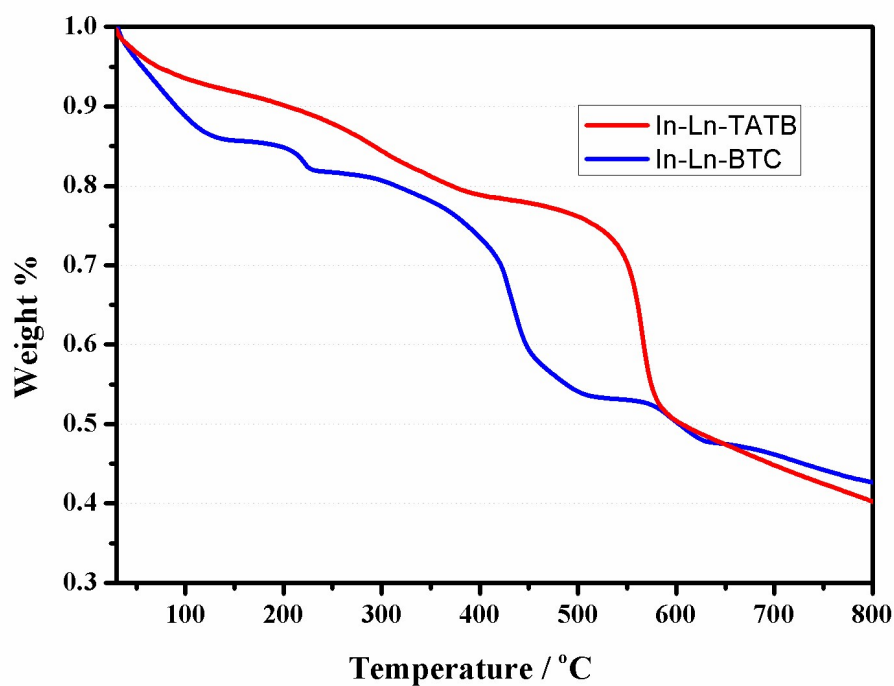


Figure S4. TGA data of **1** and **2**.

TGA analysis was carried out on a Shimadzu TGA-50 thermal analyzer through slowly heating samples from room temperature to 800°C with a rate of 10°C/min under nitrogen flow. The solvent molecules of both compounds in the channel can be easily removed from the pores below 200°C and no crystal collapse is observed. The TGA spectra show compound **1** remains stable until about 500°C, while compound **2** remains stable until about 300°C. Both compound **1** and **2** show good thermal stability.

6 ICP and EDS measurement of 1 and 2

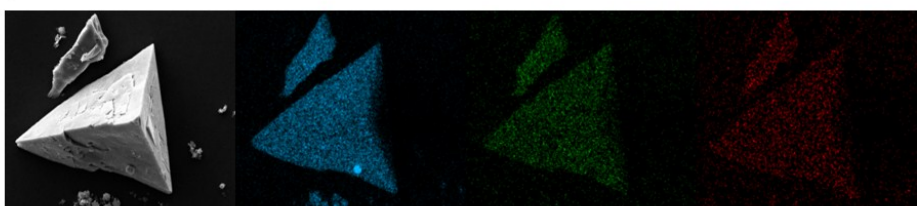
Table S1. EDS and ICP data of Tb:Eu in compound 1 and 2.

Raw ratio of Tb:Eu	Final ratio of Tb:Eu			
	EDS of 1	ICP of 1	EDS of 2	ICP of 2
1:4	1.01:4	1.03:4	1.06:4	0.97:4
2:3	1.94:3	2.05:3	1.97:3	2.02:3
1:1	1.07:1	1.03:1	1.03:1	0.98:1
3:2	3.06:2	2.99:2	3.05:2	3.02:2
4:1	3.98:1	4.03:1	3.94:1	3.95:1

We picked five groups for each compound to take EDS and ICP measurement. The EDS and ICP data show the final content can be controlled by the adding amount of raw materials.

7 EDS mapping of 2

(a)



(b)

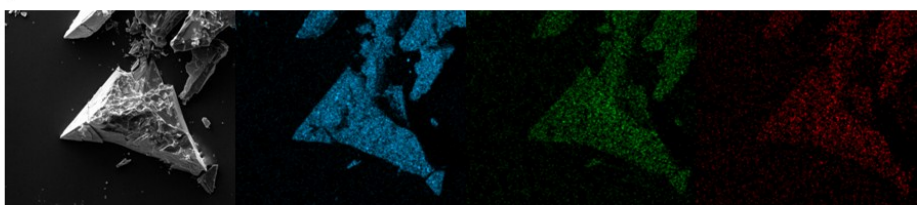


Figure S5. EDS mapping of the crystal external surface (a) and internal part (b) of 2. SEM image and corresponding element (blue: In; green: Tb; red: Eu). Scale bar: 20 μ m. The mapping data show that Eu and Tb are uniform distribution in both crystal external surface and internal part.

8 Calculating of the triplet state of TATB

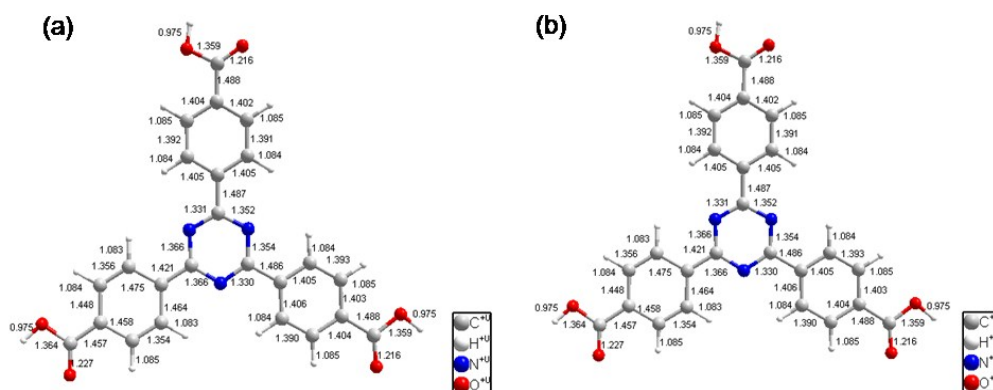


Figure S6. Optimized ground-state structure (a) and optimized triplet state structure (b) of TATB. Theoretical calculations were carried out on the Gaussian 03 equipped with Gauss View. The geometrical optimizations were performed at the B3LYP/6-31G(d) level of theory.

The calculated ground state and triplet state energy is -1539.322247 hartree and -1539.2333806 hartree, respectively. Using the equation below the triplet state of the ligand TATB can be easily obtained.

$$1 \text{ hartree} = 2625.5 \text{ kJ}\cdot\text{mol}^{-1}$$

$$1 \text{ kJ}\cdot\text{mol}^{-1} = 83.5934788 \text{ cm}^{-1}$$

9 Fluorescent photograph of **1** soaked in different organic solvents

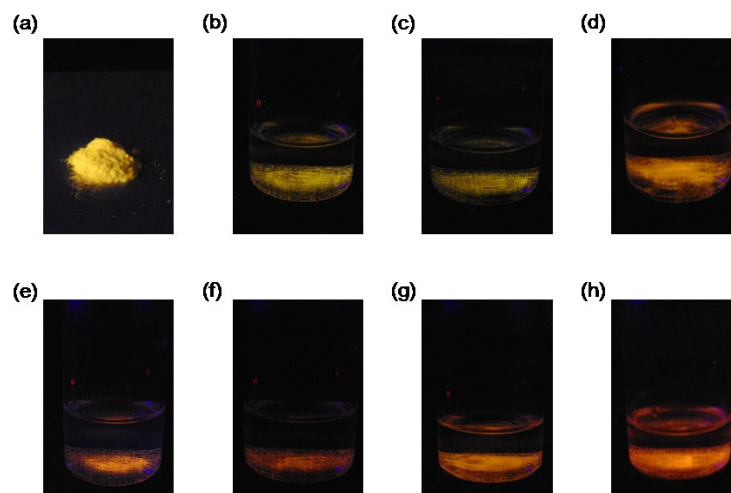


Figure S7. Photograph of **1** with the Tb:Eu ratio of 19:1 in solvent with different polarity. (a) solid-state; (b) cyclohexane; (c) CCl_4 ; (d) CHCl_3 ; (e) CH_2Cl_2 ; (f) diethyl ether; (g) THF; (h) DMF.

While soaked in solvent with low polarity, compound **1** barely changes in its luminescent color compared to the solid state. However, with the solvent polarity increasing, the luminescent color generally turns from yellow to orange-red.

10 Gas sorption measurement of compound 2

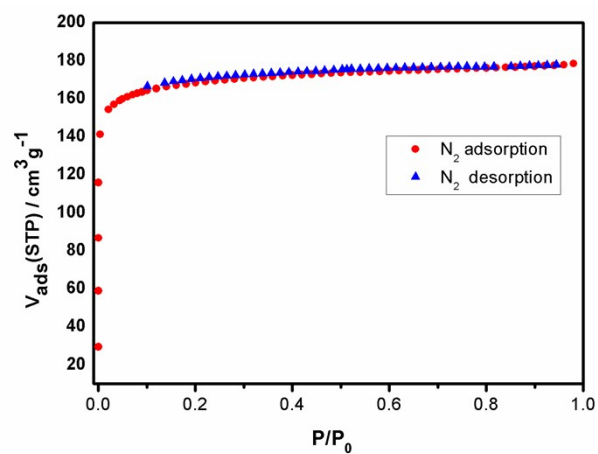


Figure S8. N_2 adsorption (red) and desorption (blue) isotherms of compound **2** at 77K.

Gas absorption of compound **1** is unavailable due to the collapse of the framework during the measurement. Only gas absorption data of compound **2** is obtained, which is close to gas absorption behavior of CPM-5 reported before.